**Iğdır Üniversitesi Fen Bilimleri Enstitüsü Dergisi, 13(4), 2829-2837, 2023**
***Journal of the Institute of Science and Technology, 13(4), 2829-2837, 2023***

**ISSN: 2146-0574, eISSN: 2536-4618**

**Chemistry** **DOI: 10.21597/jist.1294448**

**Research Article**

**Received: 09.05.2023** **Accepted: 14.06.2023**

**To Cite***:* Nas, M. S., Calimli, M. H. & Demirbaş, Ö. (2023). Fabrication of Highly Efficient $Fe_3O_4$/SSIP/GO Composite Films for Removal of Methylene Blue Dy. *Journal of the Institute of Science and Technology*, 13(4), 2829-2837.

# Fabrication of Highly Efficient $Fe_3O_4$/SSIP/GO Composite Films for Removal of Methylene Blue Dye

Mehmet Salih NAS[1*], Mehmet Harbi CALIMLI[1], Özkan DEMİRBAŞ[3]

**Highlights:**

- The composite film was synthesized by an extruder device.
- Tested optimum conditions for methylene blue removal
- Adsorption kinetics were performed using three different models

**Keywords:**

- Sunflower
- Adsorption
- Composite film
- Characterization

**ABSTRACT:**

In this paper, we report the preparation of a new $Fe_3O_4$/SSIP/GO composite film for the purification of methylene blue dye from solution media. The preparation process of composite film was carried out to improve the interaction between the inner part of the sunflower stalk (SSIP) and surface matrix using magnetite/Graphene Oxide ($Fe_3O_4$/GO) minerals at weight ratios (0.2/4/0.2:w/w/w). The characterizations of as-developed $Fe_3O_4$/SSIP/GO composite film was successfully carried out by some advanced techniques such as FT-IR, SEM, and TGA analyses. Adsorption kinetic studies were evaluated in three different aspects as a pseudo-first-order model, pseudo-second-order model, and intraparticle diffusion-type model. Based on the $R^2$ results, it was seen that the Pseudo-second order kinetic model (0.999) acted more harmoniously than the pseudo-first-order (0.960) and intra-particle diffusion technique models (0.974). In the light of these findings, it can be said that the prepared $Fe_3O_4$/SSIP/GO composite film used for removal of methylene blue dye can be considered as a promising material

.

[1] Mehmet Salih NAS (**Orcid ID:** 0000-0003-1092-5237), Mehmet Harbi CALIMLI (**Orcid ID:** 0000-0001-9756-191X), Iğdır Üniversity, Department of Medical Services and Techniques, Tuzluca Vocational School, Iğdır University, Iğdır, Türkiye.
[3] Özkan DEMİRBAŞ (**Orcid ID:** 0000-0001-9548-0227), Iğdır University, Department of Chemistry, Faculty of Science and Literature, University of Balikesir, Türkiye.

***Sorumlu Yazar/*Corresponding Author*:** Mehmet Salih NAS, e-mail: msalih.nas@igdir.edu.tr

## INTRODUCTION

The sunflower plant, which is an annual and broad-leaved species, constitutes the majority of oil resources worldwide(P. et al. 2009) (Vaithanomsat et al., 2009). Parallel to the increase in the world population, the increase in the amount of oil consumption has resulted in a positive increase in sunflower cultivation areas. After the sunflower plant is harvested, an extremely high significant amount of product is produced as as the leaves, heads and stems of the sunflower plant (Follain et al. 2015). If sunflower stalks are not well controlled, a way is followed by burning them. This method leads to environmental pollution with severe consequences and misuse of the source material (Shi and Yang, 2012). However, a high amount of pectin and cellulose is obtained by extracting sunflower stalks (SSP), and a different alternative source is gained for the obtained pectin extraction, biofuel extraction, or cellulose-based materials (Xu et al. 2020), a very large specific surface area, and a special structure compared to lignocellulosic fiber materials (Sun et al., 2013). SSP can be considered an adsorbent source for the removal of polluted wastes in wastewater due to its unique physicochemical structural properties(Oguntimein 2015; Nas 2021) , easy degradability (Jalali and Aboulghazi 2013), and cost-effectiveness (Knapik and Stopa 2018). The rapid increase in industrial activities in recent times has led to the formation of wastes that leave serious negative traces on the environmental cycle and human health. Pollutants released into the aquatic environment from different industries are the main serious factors damaging the habitat. Toxic heavy metals, dyestuffs, drugs, organic acid products, phenolic substances, and halogenated compounds are some of the pollutants that negatively pollute the environment. Even in trace amounts, these products have very serious dangerous consequences for humans and aquatic organisms. E. Pollutants have a great role in environmental pollution due to the use of textiles, paper, cosmetics, printing, medicine, food, and leather (Tang et al. 2019) . Dyestuffs in wastewater are very dangerous due to their high toxicity. In addition, since the dyes released into the environment give an undesirable color to the water, they prevent the sunlight from being taken sufficiently (Jiang et al. 2019). Before these waste materials are released into the environment, toxic and reactive dyes must be purified using appropriate processes (Nas and Kaya 2020). The adsorption process, membrane separation method, precipitation way, precipitation, ion exchange mechanism, flocculation process, electrochemistry way, photoelectrochemistry method, advanced oxidation process mechanisms (AOPs), and biological treatment method are among the most accepted methods to remove unwanted dyestuffs from the environment (Parvin et al. 2019; Wekoye et al. 2020). Among these treatment type methods, the adsorption method is the most preferred process approach due to its positive features such as being economical, easy to apply, and environmentally friendly (Cheng et al. 2017; Nas 2019; Bingül Reçber et al. 2022). In general, waste biomass products, clay-containing minerals, and activated carbon are used as a source of adsorbent material for dye removal in the adsorption process (Liu et al. 2019; Bayat et al. 2022). This study, the composite film obtained from a mixture of SSIP, $Fe_3O_4$, and GO was used as a vehicle for removing the MB dyestuff. The synthesized composite film samples were characterized by SEM, TGA, and FT-IR analysis techniques, respectively. As a result, we can say that it has been seen that it can be used effectively in the removal of pollutants such as methylene blue by using composite film in a water solution environment.

## MATERYAL VE METOT

### Chemicals

$FeCl_3.6H_2O$, $FeCl_2.4H_2O$, sodium hydroxide compound, ethanol, graphite material, and methylene blue were used from Sigma Aldrich Chemical Company. In this trial study, the inner part of the

sunflower stalk, which is used as a precursor material for dye removal, was obtained from the province of Iğdır in Turkey.

### Preparation of $Fe_3O_4$

0.2 g $FeCl_3$ and 0.08 g $FeCl_2$ were mixed in 36 mL deionized water at 50 °C for 15 minutes. Then, NaOH solution (0.1 M) prepared to the reaction medium was added dropwise until the black color disappeared (pH=9), and the solution mixture was stirred vigorously for 1 hour at room temperature. The final product was separated by a supermagnet material by thorough washing with deionized water and ethanol and allowed to dry for 2 hours in an oven at 60 °C (Wei et al. 2012).

### Preparation of graphene oxide

Graphene oxide synthesis was prepared with reference to the Hummers process (Benzait et al. 2021). The oxidation was carried out by adding sulfuric acid (360 mL) and phosphoric acid (40 mL) to the graphite flake (3 g) materials, respectively. After stirring for 30 minutes, potassium permanganate (18 g) was added to the medium and stirred for a day so that the oxidation process was efficient. Then 500 ml of water and 10 ml of hydrogen peroxide were added to this mixture. The final mixture was allowed to cool in an ice bath. Then the mixture was washed with copious amounts of HCI solution (1 M) and distilled water and left to dry in an oven at 70 °C for 12 hours.

### Preparation of $Fe_3O_4$/ SSIP /GO composites film

Before mixing, the $Fe_3O_4$, SSIP, and GO samples were dried at 105 °C for 2 hours. The products were then cooled to room temperature in a desiccator. After mixing the $Fe_3O_4$/ SSIP/GO composite film at weight ratios (0.2/4/0.2:w/w/w), they were combined in a single screw extrusion apparatus. Composite film was made at a temperature range of 140-170 °C and a screw speed of 15 rpm.

### Characterization of prepared composite films

Fourier transforms infrared (FTIR) spectrum measurements of the materials prepared with SSIP, GO, and $Fe_3O_4$/SSIP/GO, a Perkin Elmer Spectrum brand device was used by taking the wavelength range of 2500-400 as reference. Thermogravimetric measurements and differential thermal analyzes (TG/DTA) of the prepared samples were performed by taking the 25–800 ˚C temperature range as a reference, taking into account the 15◦/min heating rate and nitrogen atmosphere. The morphological structures of the targeted products were analyzed using a scanning electron microscope (SEM) device.

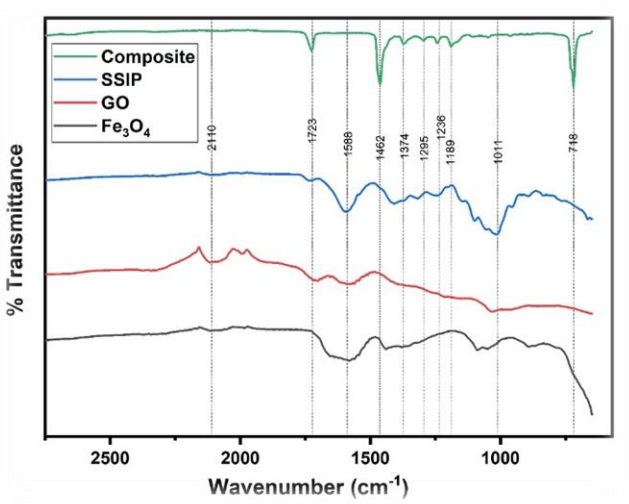


**Figure 1.** FTIR spectrum of $Fe_3O_4$, GO, SSIP and $Fe_3O_4$/ SSIP/GO

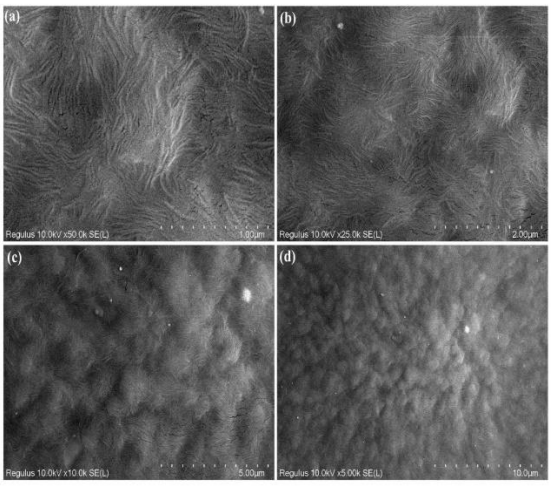


**Figure 2.** SEM pattern of $Fe_3O_4$/ SSIP/GO

## Adsorption test process of methylene blue

Adsorption test analyses are performed by setting up a three-necked laboratory-type glass balloon setup. Methylene blue stock solutions were prepared using the specified amount of distilled water as solvent. Experimental run analyzes were performed at room temperature at a stirring speed of 400 rpm (pH 9) at initial concentration conditions of 5 x $10^{-6}$ M methylene blue. The effect of the prepared composite films on the dye removal was tested in a time interval of 1440 minutes and at 400 rpm. It was done using NaOH solution (0,1 M) and HCl solution (0,1 M) to adjust the pH of the methylene blue solution. 3 mL sample was taken from the solution to interpret each adsorption assay. These samples were centrifuged at 5000 rpm (Cary 1E UV-Vis spectrophotometer) for 5 minutes. Adsorption data were instantaneously followed and determined using Equation (1) to test the amount of methylene blue absorbed on the composite film surface as shown below.

$$qt = \frac{(Co-Ce)}{m} \times V \quad (1)$$

where qt is the initial amount of the adsorbent dyestuff type, Co is the amount of the initial MB concentration value used, Ct is the amount of the MB concentration value at any point, m is the mass of the supporting material type used and V is the volume of the solution used in the process. (Demirbaş et al. 2002).

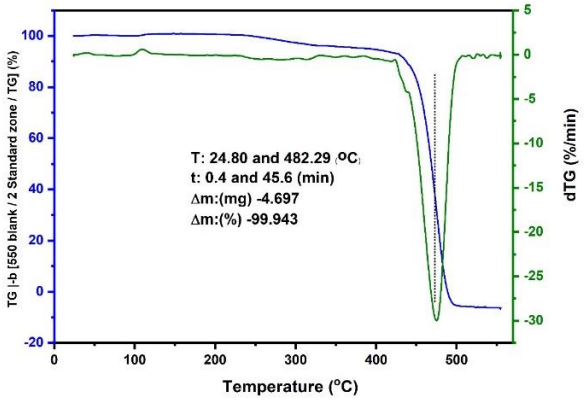


**Figure 3.** TGA curve of $Fe_3O_4$/ SSIP/GO

## BULGULAR VE TARTIŞMA

### Investigation of the morphological and chemical structure of the composite film

The FT-IR spectrum of $Fe_3O_4$, GO, SSIP, and $Fe_3O_4$/SSIP/GO composite film particles is imaged in Figure 1. The band peak at 1588 $cm^{-1}$ in the FTIR spectrum of SSIP indicates the C—O stretch

vibration peaks of aromatic carbonyl groups C=O, and C=C groups in the raw spectrum. Band peak values close to 1425 $cm^{-1}$ represent the $CH_2$ asymmetric deformation state and the variation due to aromatic C–C stretching. The peak band values observed between 1390 and 1011 $cm^{-1}$ represent the peaks associated with carboxylic acids, alcohols, esters, and phenolic compounds in lignin (O–H bending, C–O stretching). In the structure of cellulose and hemicellulose, a peak state of C–O–C stretching appeared at 1050 $cm^{-1}$ (Podder & Majumder, 2015). Peak band status was observed between 900 and 600 $cm^{-1}$ due to antisymmetric out-of-plane aromatic ring stretching (Baysal et al., 2018). SEM device was used to define the surface morphology of the targeted materials. The variation in the morphology of the doped iron oxide compound, GO, and crude SSIP were explained using SEM images of samples at different nanoscales in Figure 2. TGA analysis results are given regarding the samples' thermal degradation and mass losses. TGA results were used with the Perkin Elmer Pyres model analyzer. The $Fe_3O_4$/SSIP/GO composite film was analyzed at 0–500 °C. As indicated in Figure 3, all TGA analysis results were performed in a nitrogen gas environment and at a heating rate of 10 °C/min. $Fe_3O_4$/SSIP/GO composite film was synthesized using weight ratios (0.2/4/0.2:w/w/w) forming a homogeneous mixture. According to the TG/DTA curves of the Fe3O4/SSIP/GP composite film, it is seen that a two-step reaction interaction occurs. The composite film is resistant to temperatures up to 482 degrees, and it was noticed that if it was above this degree, it lost its strength at a high rate and its structure deteriorated. Therefore, a high rate of mass loss was observed.

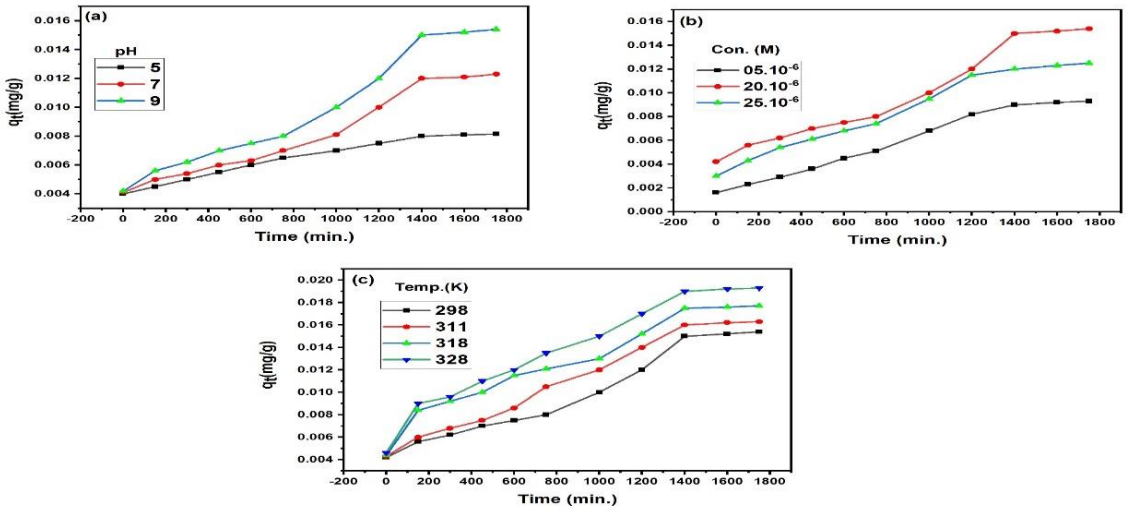


**Figure 4.** (a) Effect adsorption of pH to MB removal (b) Effect adsorption of initial dye concentration to MB removal (c) Effect adsorption of temperature to MB removal

## Effect of diferent pH on adsorption kinetics

The variation of the adsorption kinetics of the dye solution at different pH ranges is given in Figure 4(a). As the pH increased, the amount of adsorption increased. Generally, there are both negatively and positively charged functional groups on the surface of the composite film used in adsorption kinetic studies (Nandi et al. 2009). The effect of removing methylene blue (MB) from the water solution with the composite film was tested in the pH range of 5-9. The hydrophobic functional groups on the composite film surface interact with MB (Ghaedi et al. 2015). The datas obtained from this result show the presence of very strong electrostatic forces between the positively charged MB and the negative density composite film when the pH value of the solution increases (Li et al. 2010; Çalımlı et al. 2019; Demirbaş et al. 2019).

## Effect of dye concentration on adsorption results

Determination of the adsorption effect on MB dye concentration was tested by preparing samples of different concentrations of $0.5.10^{-5}$-$2.5.10^{-5}$ M. Experimental analyses in the presence of a contact time of 1440 minutes, pH 7, and a temperature of 25 ˚C**.** Increasing the MB dye concentration from $0,5.10^{-5}$ M to $2,5.10^{-5}$ M resulted in a negative synergistic resulting in a decrease in adsorption efficiency from 90% to 75%. The density of the pore areas available on the composite film is sufficient to adsorb a certain of dyestuff in concentration. The increase in dyestuff concentration above this value is not sufficient for adsorbing. In this case, it causes a slight decrease in the MB removal (Figure 4(b)).

**Effect of temperature parameter on adsorption Kinetics**

In Figure 4(c), the adsorption kinetic change was tested under constant conditions determined at different temperatures. It has been observed that the temperature function is quite effective in the removal of MB dye adsorption on the composite film. Experimental studies were performed at 25, 38, 45, and 55 °C using pH 9 and $20\times10^{-6}$ M initial methylene blue concentration constant conditions. It was determined that the best efficiency adsorption amount was obtained at 55 °C. This situation can be explained as follows. As the temperature increases, the adsorption value equivalent to the diffusion rate of the molecules on the composite film increases due to the increase in the kinetic energies of the molecules. The pores of the composite film increase in volume depending on the temperature increase. This creates a positive synergistic effect on the adsorption value of MB removal (Dahri et al. 2015). In addition, an image is shown in a lab-tested working example of MB dye removal with composite film ( Figure 5) (Şen et al. 2018).

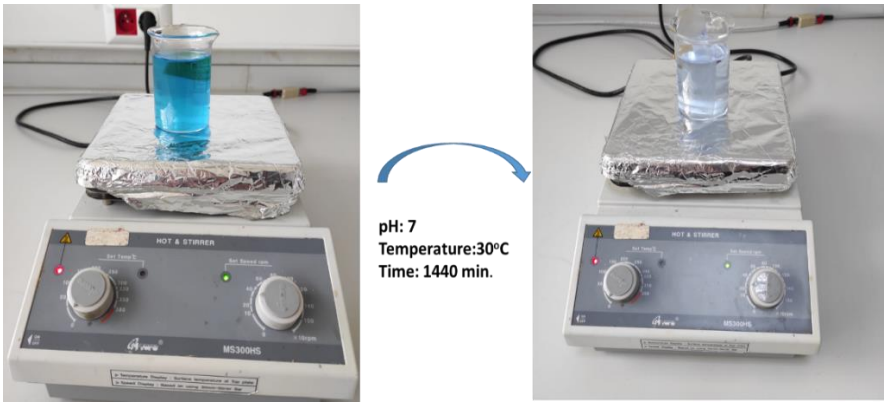


**Figure 5.**A lab-tested image of MB dye removal with $Fe_3O_4$/SSIP/GO composite film

**Adsorption kinetics**

Adsorption kinetics were tested using the following formulas of pseudo-first-order, pseudo-second-order, and intra-particle diffusion model. Based on the $R^2$ results, it was seen that the Pseudo-second order kinetic model (0.999) acted more harmoniously than the pseudo-first-order (0.660) and intra-particle diffusion model (0.974)

$$\ln(q_e-q_t) = \ln q_e - k_i t \quad (2)$$

$$\frac{t}{qt} = \frac{1}{k_2 q_e^2} + \frac{1}{q_e} t \quad (3)$$

$$q_t = k_{int} t_{1/2} + C \quad (4)$$

Where; the t , $q_e$, $q_t$, $k_2$ and $k_{int}$ (mg (g $min^{-1/2}$)$^{-1}$ is time (min.), first amount of MB, last amount of MB, and the constant ratios, respectively (Ho and McKay 1999; Demirbaş et al. 2014) .

**Tablo 1**. Isotherm models used for testing adsorption kinetics

| Isotherm Model | Model Equation | Parameters | Değişken sabitler |
|---|---|---|---|
| Freundlich | $\log(qe) = logKF + \frac{1}{n} logCe$ | $R^2$=0.996 | **$K_F$**:Freundlich isotherm constant<br>**n**:Adsorption intensity |
| Langmuir | $\frac{Ce}{qe} = \frac{1}{K_L(qmax.)} + \frac{Ce}{qmax.}$ | $R^2$=0,948 | **$K_L$**:Langmuir isotherm cons.<br>**qmax**.:maximum adsoprtion capacity |
| Temkin | $qe = \frac{RT}{b}(lnKT + lnCe)$ | $R^2$=0.964 | **b:**Temkin isotherm cons.<br>**$K_T$**:Temkin isotherm binding cons. |

Langmuir, Freundlich, and Temkin adsorption isotherm models were tested to investigate adsorption isotherms. The isotherm parameters of the adsorption are detailed in Table 1. Based on the $R^2$ results, it was found to be more compatible than the Freundlich (0.996), Langmuir (0.948), and Temkin (0.964) isotherm models.

## CONCLUSION

Composite film consisting of $Fe_3O_4$/SSIP/GO was successfully prepared and applied to investigate the methylene blue removal efficiency. The kinetic parameters (temperature, initial concentration of methylene blue, and pH) of the adsorption between the $Fe_3O_4$/SSIP/GO composite film and methylene blue were analyzed. Experimental datas showed that increasing methylene blue concentration has a positive synergistic effect on adsorption efficiency. In addition, it was determined that the adsorption increased when the pH values of the prepared dye solution increased from 5 to 9. Adsorption kinetic studies were carried out at temperatures, contact times, and pH conditions, which determined the adsorption mechanism and isotherm model. As a result of the calculations, it was determined that there is a positive relationship consistent with the adsorption kinetic datas of MB on the $Fe_3O_4$/SSIP/GO composite film surface, Freundlich isotherm ($R^2$ =0.996) and the pseudo-second-order kinetic process model ($R^2$ =0.999). In this study, we can say that $Fe_3O_4$/SSIP/GO composite film can be preferred as an effective adsorbent for dye removal.

## TEŞEKKÜR

This study was funded by Iğdır University Scientific Research Projects Commission (No: MÜF0520A12).

### Çıkar Çatışması

The article authors declare that there is no conflict of interest between them.

### Yazar Katkısı

The authors declare that they have contributed equally to the article.

## KAYNAKLAR

Bayat, R., Bingül Reçber, Z., Bekmezci, M., Nas, M. S., Calimli, M. H., Demirbas, O., Akin, M., & Şen, F. (2022). Synthesis and application of AuNi@AC nano adsorbents for the removal of Maxilon Blue 5G azo dye from aquatic mediums. *Food and Chemical Toxicology*, *167*, 113303. https://doi.org/10.1016/J.FCT.2022.113303

Baysal, M., Bilge, K., Yılmaz, B., Papila, M., & Yürüm, Y. (2018). Preparation of high surface area activated carbon from waste-biomass of sunflower piths: Kinetics and equilibrium studies on the dye removal. *Journal of Environmental Chemical Engineering*, *6*(2), 1702–1713. https://doi.org/10.1016/J.JECE.2018.02.020

Benzait, Z., Chen, P., & Trabzon, L. (2021). Enhanced synthesis method of graphene oxide. *Nanoscale Advances*, *3*(1), 223–230. https://doi.org/10.1039/D0NA00706D

Bingül Reçber, Z., Burhan, H., Bayat, R., Nas, M. S., Calimli, M. H., Demirbas, Ö., Şen, F., & Hassan, K. M. (2022). Fabrication of activated carbon supported modified with bimetallic-platin ruthenium nano sorbent for removal of azo dye from aqueous media using enhanced ultrasonic wave. *Environmental Pollution*, *302*, 119033. https://doi.org/10.1016/J.ENVPOL.2022.119033

Çalımlı, M. H., Demirbaş, Ö., Aygün, A., Alma, M. H., Nas, M. S., Khan, A., Asiri, A. M., & Şen, F. (2019). Equilibrium, Kinetics and Thermodynamics of Bovine Serum Albumin from Carbon Based Materials Obtained from Food Wastes. *BioNanoScience*, *9*(3), 692–701. https://doi.org/10.1007/S12668-019-00633-Z

Cheng, S., Zhang, L., Xia, H., Peng, J., Shu, J., Li, C., Jiang, X., & Zhang, Q. (2017). Adsorption behavior of methylene blue onto waste-derived adsorbent and exhaust gases recycling. *RSC Advances*, *7*(44), 27331–27341. https://doi.org/10.1039/C7RA01482A

Dahri, M. K., Kooh, M. R. R., & Lim, L. B. L. (2015). Original Article. *Alexandria Engineering Journal*, *4*(54), 1253–1263. https://doi.org/10.1016/J.AEJ.2015.07.005

Demirbaş, O., Alkan, M., & Doğan, M. (2002). The removal of victoria blue from aqueous solution by adsorption on a low-cost material. *Adsorption*, *8*(4), 341–349. https://doi.org/10.1023/A:1021589514766/METRICS

Demirbaş, Ö., Çalımlı, M. H., Demirkan, B., Alma, M. H., Nas, M. S., Khan, A., Asiri, A. M., & Şen, F. (2019). Thermodynamics, Kinetics, and Adsorption Properties of Biomolecules onto Carbon-Based Materials Obtained from Food Wastes. *BioNanoScience*, *3*(9), 672–682. https://doi.org/10.1007/S12668-019-00628-W

Demirbaş, Ö., Turhan, Y., & Alkan, M. (2014). Thermodynamics and kinetics of adsorption of a cationic dye onto sepiolite. *New Pub: Balaban*, *54*(3), 707–714. https://doi.org/10.1080/19443994.2014.886299

Follain, N., Saiah, R., Fatyeyeva, K., Randrianandrasana, N., Leblanc, N., Marais, S., & Lecamp, L. (2015). Hydrophobic surface treatments of sunflower pith using eco-friendly processes. *Cellulose*, *22*(1), 245–259. https://doi.org/10.1007/S10570-014-0490-1

Ghaedi, M., Hajjati, S., Mahmudi, Z., Tyagi, I., Agarwal, S., Maity, A., & Gupta, V. K. (2015). Modeling of competitive ultrasonic assisted removal of the dyes – Methylene blue and Safranin-O using Fe3O4 nanoparticles. *Chemical Engineering Journal*, *268*, 28–37. https://doi.org/10.1016/J.CEJ.2014.12.090

Ho, Y. S., & McKay, G. (1999). Pseudo-second order model for sorption processes. *Process Biochemistry*, *34*(5), 451–465. https://doi.org/10.1016/S0032-9592(98)00112-5

Jalali, M., & Aboulghazi, F. (2013). Sunflower stalk, an agricultural waste, as an adsorbent for the removal of lead and cadmium from aqueous solutions. *Journal of Material Cycles and Waste Management*, *15*(4), 548–555. https://doi.org/10.1007/S10163-012-0096-3/TABLES/5

Jiang, C., Wang, X., Qin, D., Da, W., Hou, B., Hao, C., & Wu, J. (2019). Construction of magnetic lignin-based adsorbent and its adsorption properties for dyes. *Journal of Hazardous Materials*, *369*, 50–61. https://doi.org/10.1016/J.JHAZMAT.2019.02.021

Knapik, E., & Stopa, J. (2018). Fibrous deep-bed filtration for oil/water separation using sunflower pith as filter media. *Ecological Engineering*, *121*, 44–52. https://doi.org/10.1016/J.ECOLENG.2017.07.021

Li, Y., Liu, F., Xia, B., Du, Q., Zhang, P., Wang, D., Wang, Z., & Xia, Y. (2010). Removal of copper from aqueous solution by carbon nanotube/calcium alginate composites. *Journal of Hazardous Materials*, *177*(1–3), 876–880. https://doi.org/10.1016/J.JHAZMAT.2009.12.114

Liu, J., Wang, N., Zhang, H., & Baeyens, J. (2019). Adsorption of Congo red dye on FexCo3-xO4 nanoparticles. *Journal of Environmental Management*, *238*, 473–483. https://doi.org/10.1016/J.JENVMAN.2019.03.009

Nandi, B. K., Goswami, A., & Purkait, M. K. (2009). Adsorption characteristics of brilliant green dye on kaolin. *Journal of Hazardous Materials*, *161*(1), 387–395. https://doi.org/10.1016/J.JHAZMAT.2008.03.110

Nas, M. S. (2021). AgFe2O4/MWCNT nanoparticles as novel catalyst combined adsorption-sonocatalytic for the degradation of methylene blue under ultrasonic irradiation. *Journal of Environmental Chemical Engineering*, *9*(3), 105207. https://doi.org/10.1016/J.JECE.2021.105207

Nas, M. S., & Kaya, H. (2020). Synthesis and sonocatalytic performance of bimetallic AgCu@MWCNT nanocatalyst for the degradation of methylene blue under ultrasonic irradiation. *Https://Doi.Org/10.1080/24701556.2020.1799406*, *51*(5), 614–626. https://doi.org/10.1080/24701556.2020.1799406

Nas, M. salih. (2019). The Investigation of Thermodynamics Parameters and Adsorption Kinetic of The Maxilon Blue 5G Dye on Turkey Green Clay. *Journal of the Institute of Science and Technology*, 749–758. https://doi.org/10.21597/JIST.475791

Oguntimein, G. B. (2015). Biosorption of dye from textile wastewater effluent onto alkali treated dried sunflower seed hull and design of a batch adsorber. *Journal of Environmental Chemical Engineering*, *3*(4), 2647–2661. https://doi.org/10.1016/J.JECE.2015.09.028

P., V., S., C., & W., A. (2009). *Bioethanol production from enzymatically saccharified sunflower stalks using steam explosion as pretreatment*. https://ir.swu.ac.th/jspui/handle/123456789/15454

Parvin, S., Biswas, B. K., Rahman, M. A., Rahman, M. H., Anik, M. S., & Uddin, M. R. (2019). Study on adsorption of Congo red onto chemically modified egg shell membrane. *Chemosphere*, *236*, 124326. https://doi.org/10.1016/J.CHEMOSPHERE.2019.07.057

Podder, M. S., & Majumder, C. B. (2015). SD/MnFe2O4 composite, a biosorbent for As(III) and As(V) removal from wastewater: Optimization and isotherm study. *Journal of Molecular Liquids*, *212*, 382–404. https://doi.org/10.1016/J.MOLLIQ.2015.09.011

Şen, F., Demirbaş, Ö., Çalımlı, M. H., Aygün, A., Alma, M. H., & Nas, M. S. (2018). The dye removal from aqueous solution using polymer composite films. *Applied Water Science*, *8*(7). https://doi.org/10.1007/S13201-018-0856-X

Tang, S., Xia, D., Yao, Y., Chen, T., Sun, J., Yin, Y., Shen, W., & Peng, Y. (2019). Dye adsorption by self-recoverable, adjustable amphiphilic graphene aerogel. *Journal of Colloid and Interface Science*, *554*, 682–691. https://doi.org/10.1016/J.JCIS.2019.07.041

Wei, Y., Han, B., Hu, X., Lin, Y., Wang, X., & Deng, X. (2012). Synthesis of Fe3O4 Nanoparticles and their Magnetic Properties. *Procedia Engineering*, *27*, 632–637. https://doi.org/10.1016/J.PROENG.2011.12.498

Wekoye, J. N., Wanyonyi, W. C., Wangila, P. T., & Tonui, M. K. (2020). *Kinetic and equilibrium studies of Congo red dye adsorption on cabbage waste powder*. https://doi.org/10.1016/j.enceco.2020.01.004

Xu, M., Qi, M., Goff, H. D., & Cui, S. W. (2020). Polysaccharides from sunflower stalk pith: Chemical, structural and functional characterization. *Food Hydrocolloids*, *100*, 105082. https://doi.org/10.1016/J.FOODHYD.2019.04.053